Micromechanical Model for Deformation in Solids with Universal Predictions for Stress-Strain Curves and Slip Avalanches

Karin A. Dahmen, Yehuda Ben-Zion, and Jonathan T. Uhl

Department of Physics, University of Illinois at Urbana Champaign, Urbana, Illinois 61801, USA, and Department of Earth Sciences, University of Southern California, Los Angeles, California 90089-0740, USA

(Received 23 May 2008; published 27 April 2009)

A basic micromechanical model for deformation of solids with only one tuning parameter (weakening ε) is introduced. The model can reproduce observed stress-strain curves, acoustic emissions and related power spectra, event statistics, and geometrical properties of slip, with a continuous phase transition from brittle to ductile behavior. Exact universal predictions are extracted using mean field theory and renormalization group tools. The results agree with recent experimental observations and simulations of related models for dislocation dynamics, material damage, and earthquake statistics.

DOI: 10.1103/PhysRevLett.102.175501 PACS numbers: 62.20.fq, 91.30.Px

Plastic and brittle deformations of solids have been studied in various scientific disciplines for more than a century, and many important results have been obtained in the past [1]. Initially plastic deformation was modeled as a smooth, continuous deformation of nominally homogeneous materials. However, recent experiments [1,2] on small nickel crystals and other materials reveal steplike stress-strain curves with broad power-law-distributed dislocation slip avalanches and the formation of slip-bands on the sample surface. The power law relationship between frequency and event size has been shown to be material independent (i.e. ''universal''). The same is true for the geometric roughness of slip surfaces and related quantities. The process looks remarkably similar to the brittle deformation of the earth's crust with Gutenberg Richter power law statistics of earthquake sizes and fractal-like fault networks [1–3]. To quantify the analogies, we introduce a basic micromechanical model with threshold dynamics for deformation in crystals, which shows richer dynamics than many traditional continuum models. An important advantage of this model is that it has very few ingredients and yet is able to provide exact quantitative predictions for universal scaling properties that correctly reproduce many essential features of the dynamics. Using only one tuning parameter (weakening ε), it yields a surprisingly general understanding of the universal long length scale behavior of multiple types of deformation responses (brittle, ductile, or hardening) seen in laboratory experiments. Another advantage is that it provides *exact* analytical results and quantitative predictions for universal scaling forms, exponents, and functions that can be measured in experiments. Tools from the theory of phase transitions and the renormalization group are used to calculate exact material independent (universal) scaling predictions for a large range of scales: scaling results for stress-strain curves, noise power spectra, slip pulse size, duration distributions, and geometrical properties are computed exactly for two different types of boundary conditions (a slowly increasing applied shear stress or a small fixed tangential boundary velocity). For slowly increasing applied shear stress the results agree with recent experiments and simulations [1]. New experiments are suggested to test new exact predictions. For the fixed velocity boundary condition, the model results agree with those for two related earthquake models [4,5]. The discussed framework thus represents a generalization of recent models for dislocation dynamics [1] and may be used to understand the similarities and differences between models for deformation of solids and models for earthquake dynamics.

The model.—Consider a three-dimensional block of material that deforms under shear. On a large scale it may represent an entire crustal region, without a preexisting dominant crack or fault [5]. Two different boundary conditions are applied:

(I) A slowly increasing shear stress F applied to the boundaries, or

(II) A small tangential velocity v imposed at the boundaries.

The local medium behaves elastically until the static local failure stress $\tau_{s,r}$ is exceeded. It then undergoes a local slip until the local shear stress is reduced to a lower arrest stress $\tau_{a,r}$ (''sticking stress''). $\tau_{s,r}$ and $\tau_{a,r}$ may vary with position $\mathbf{r}$, due to disorder in the system, such as stepovers, asperities in earthquake systems, or impurities and crystal imperfections in metals. The exact shape of their distribution does not affect the universal scaling results reported below. In the following we set $\tau_{a,r} = 0$ and assume a narrow parabolic distribution for $\tau_{s,r}$ [4]. After the medium sticks back together it locally acts elastically until the local stress again exceeds the current failure stress, which may have changed since the initial slip via weakening or strengthening. Each slip produces an unisotropic redistribution of elastic forces that fall off roughly as $1/D^3$ (or $1/D^2$ in two dimensions) with the distance D from the slip location. The stress redistribution takes place with the speed of sound, i.e., much faster than the (lab or

geological) time scale involved in the buildup of the stress. The slip at one point may increase the stress at other points enough to cause them to slip as well, and thus lead to an avalanche of slip instabilities, which is the analogue of an earthquake on crustal scales. An avalanche stops when at each point in the system the stress is lower than its current failure stress. The size s of each avalanche is quantified by its potency, which is the integral of the slip distance over the failure area [6]. A given slip location may experience more than one slip during an avalanche. For brittle materials, we assume that after a point r slips for the first time during an avalanche, the failure threshold at that location will be weakened from the static value $\tau_{s,r}$ to a diminished value $\tau_{d,r}$ with $\tau_{a,r} < \tau_{d,r} < \tau_{s,r}$. The failure stress remains at $\tau_{d,r}$ for the secondary and all later slips during the same avalanche. The amount of weakening is given by the weakening parameter $\varepsilon = (\tau_{s,r} - \tau_{d,r})/\tau_{s,r}$ [7]. After the completion of an avalanche all diminished failure stresses are reset to their initial static values $\tau_{s,r}$. In contrast, for hardening materials we assume that each slip event during an avalanche leads to a strengthening of all other failure thresholds by an amount proportional to $|\varepsilon|/N$, where $\varepsilon < 0$ and N is the volume of the system, to model the local energy absorption due to dislocation pair creation, entanglement, etc. [1]. For initial analysis, we study the scalar version of this model, which describes a crystal with parallel straight edge dislocations extended in the z direction. In this case, slip events are local tears in the crystal structure. They are either due to the creation of dislocation pairs (''dipoles'') or dislocation motion along the shear direction x. The local displacement discontinuity $u(\mathbf{r}, t)$ across the slip surface [4] (parallel to the xz-crystal plane), is constant along the z direction, and is related to the number of dislocations that have moved past point $\mathbf{r} = (x, y)$ by time t.

Justification for the use of mean field theory.—We use the general equations of motion [4]:

$$\eta \partial u(\mathbf{r}, t)/\partial t = F + \sigma_{\text{int}}(\mathbf{r}, t) - f_R[u, \mathbf{r}, \{u(\mathbf{r}, t' < t)\}], \tag{1}$$

where

$$\sigma_{\text{int}}(\mathbf{r}, t) = \int_{-\infty}^{t} dt' \int d^2 r' J(\mathbf{r} - \mathbf{r}', t - t') \times [u(\mathbf{r}', t') - u(\mathbf{r}, t)] \tag{2}$$

is the shear stress accumulated at point $\mathbf{r}$ at time t due to elastic stress transfer from all previous slips in the solid since time $t = 0$ when the system started in a relaxed state. Using scalar elasticity, F is the applied shear stress in the x direction (corresponding to σ_{xz} in tensor elasticity). Equation (1) provides a general description of particle motion in an environment (e.g., elastic solid) with distributed rather than concentrated mass [1]. f_R represents the quenched random ''pinning'' stress, that prevents slips until the local stress exceeds the local failure threshold, as discussed above. A renormalization group analysis of the model shows that the coupling between slips due to dislocation motion is so long range [$J(\mathbf{r}) \equiv \int dt J(\mathbf{r}, t) \sim \mathbf{r}^{-2}$ for parallel straight edge dislocations] that mean field theory (MFT) gives the correct scaling behavior in all dimensions for $\varepsilon = 0$ or ε close to zero. This agrees with a conjecture mentioned in [1] for a different model. In MFT the coupling is replaced by a function that is constant in space: $J(\mathbf{r}) \equiv J/N$ and all spatial dependence is lost. For slow driving the problem reduces to the same mean field theory as that of the Ben-Zion and Rice (BZR) model for a *single* fault driven with slow velocity boundary condition (II). The long term model behavior (i.e., for long enough time so that all memory of the initial conditions is lost) is discussed in [4,7–9]. To summarize, the main parameters of the model are as follows: ε, the boundary conditions, $\tau_{s,r}$, $\tau_{a,r}$ and their distributions, the values of η and elastic constants, and the form of $J(\mathbf{r}, t)$. Among these, only ε, the range of $J(\mathbf{r}, t)$ and the boundary conditions affect the universal aspects of the behavior on long length scales.

Exact results for a slowly increasing applied shear stress F.—In a *discrete* version of MFT with N lattice points, the local stress τ_ℓ at a lattice point ℓ is given by $\tau_\ell = J/N \Sigma_m (u_m - u_\ell) + F$ [8]. Each point fails when the stress is bigger than the local failure threshold (slip stress) $\tau_{f,\ell} \equiv \tau_{s,\ell}$ (or $\tau_{d,\ell}$). When site ℓ fails, it slips by a certain amount Δu_ℓ resulting in a stress reduction $\tau_{f,\ell} - \tau_{a,\ell} \sim 2G\ \Delta u_\ell$ where $G \sim J$ is the elastic shear modulus.

For zero weakening ($\varepsilon = 0, \tau_{s,\ell} = \tau_{d,\ell}$).—Starting from a relaxed (zero stress) state, the external stress F is increased, and the system approaches a ''depinning transition'' at the critical yield stress F_c, which has been studied previously in other contexts [4,10,11]. The stress-strain curve for this case is shown in Fig. 1. (Here the strain is proportional to $\Sigma_m u_m$). For a slowly increasing $F < F_c$, the solid responds with slip avalanches (strain steps) of size s (potency per volume) that lead to acoustic emission. At the yield stress F_c, the distribution $D(s, F_c)$ of slip avalanche sizes follows a universal power law $D(s, F_c) \sim 1/s^\tau$ with a universal critical exponent $\tau = 1.5$. Below but close to F_c, the distribution follows the same power law up to a maximum size $s_{\max} \sim (F_c - F)^{1/\sigma}$, with a universal exponent $\sigma = 0.5$. This is reflected by the large s scaling form: $D(s, F) \sim 1/s^\tau \mathcal{D}[s \cdot (F_c - F)^{1/\sigma}]$ with universal cutoff scaling function $\mathcal{D}(x) \sim A \exp(-Bx)$. The constants A and B are nonuniversal. The local slope of the stress-strain curve (the effective shear modulus G) is inversely proportional to the mean avalanche size $\langle s \rangle$; i.e., it scales as $G \sim 1/\langle s \rangle \sim (F_c - F)^{(2-\tau)/\sigma} \sim (F_c - F)$ [1,10].

Above yielding ($F > F_c$) all points keep slipping with a mean slip rate that scales as $d\langle u \rangle/dt \sim (F - F_c)^\beta$ with a universal exponent $\beta = 1$ [11]. The above analytical predictions agree with simulation results of a slightly different model for dislocation dynamics [1].

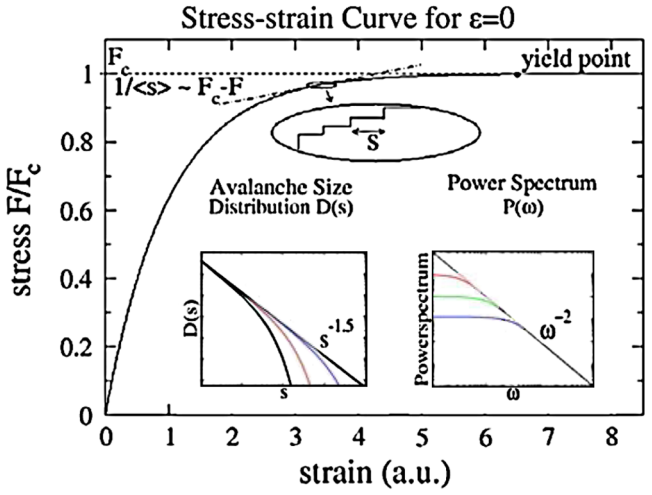

FIG. 1 (color online). Stress-strain curve for $\varepsilon = 0$ in MFT for slowly increasing applied shear stress. The two insets show log-log plots of the avalanche size distribution $D(s)$ and the power spectrum $P(\omega)$: the four size distributions arranged from left to right and the power spectra arranged from bottom to top are obtained from four different, narrow stress windows that are centered around stresses $0 < F_1 < F_2 < F_3 < F_4 = F_c$, respectively. Note how both $D(s)$ and $P(\omega)$ approach power law scaling as $F \to F_c$.

At F_c we predict the slip-rate power spectra $P(\omega, F_c)$ [i.e., the absolute square of the Fourier transform of the time dependent slip rate $d(\Sigma_m u_m)/dt$] to scale with frequency ω as $P(\omega, F_c) \sim \omega^{-2}$. For $F < F_c$ the power law levels off at frequencies below a cutoff $\omega_{\min} \sim (F_c - F)^{\nu z}$ with $\nu z = 1$. This is captured by the functional form $P(\omega, F) \sim \omega^{-2}\mathsf{fcn}[\omega/(F_c - F)]$ where $\mathsf{fcn}(x)$ is a universal scaling function. The insets of Fig. 1 show $D(s, F)$ and $P(\omega, F)$ at various stresses F. Note the respective power law scaling regimes with crossover to a stress dependent large avalanche cutoff and a low frequency cutoff for $D(s, F)$ and $P(\omega, F)$, respectively [10]. Predictions can also be made for the roughness on the surface of the deforming material and for the average amount of slip at a slipping site $\langle u \rangle_s$ for an avalanche of size s: $\langle u \rangle_s \sim s^{\zeta \sigma \nu} \sim s^0$ since $\zeta = 0$ [1,4]. The distribution of avalanche durations T is expected to scale as $D(T) \sim 1/T^{\alpha}\mathcal{D}[T(F_c - F)^{\nu z}]$ with $\alpha = 2$, $\nu z = 1$, and $\mathcal{D}(x)$ a universal scaling function. For $\varepsilon = 0$ the slip in the system is, on average, distributed uniformly over the sample (ductile deformation). Simulations of the slip distribution of two similar models [1,5] indicate that the average propagation direction of individual slip avalanches tends to be parallel to the shear direction. Chen *et al.* [5] conjectured that adding weakening to their model would lead to slip localization.

Results for weakening (*with* $\varepsilon > 0$, $\tau_{s,\ell} > \tau_{d,\ell}$).—For $\varepsilon > 0$ we find scaling behavior similar to the $\varepsilon = 0$ case prior to macroscopic failure. Here the deformation mode is different and is associated with brittle failure. Starting from a relaxed state, initially the material responds to an increasing shear stress $F < F_c(\varepsilon)$ with small avalanches, just as in the $\varepsilon = 0$ case. Their sizes are power-law distributed up to a stress dependent cutoff size $s_{\max} \sim \varepsilon^{-2}\mathsf{S}((F_c - F)/\varepsilon)$. They are nucleated randomly throughout the system and thus lead, on average, to a uniform strain distribution across the sample, similar to the situation for zero weakening. The scaling form of the avalanche size distribution in this regime, for example, is given by $D(s) \sim 1/s^{\tau} D_w[s \cdot (F_c - F)^{1/\sigma}, s \cdot \varepsilon^2]$, with the same values $\tau = 1.5$ and $1/\sigma = 2$ as in the zero weakening case. The yield stress $F_c(\varepsilon)$, is of order ε lower than the yield stress F_c for $\varepsilon = 0$ [4]. At $F_c(\varepsilon) \equiv F_c - O(\varepsilon)$ the material breaks in brittle failure; i.e., the slip suddenly localizes in a system spanning avalanche that forms a narrow weakened failure or "fault zone." The shear modulus just before failure is $G \sim O(\varepsilon)$. The system undergoes a discontinuous (first order) transition at $F_c(\varepsilon)$. (Note that MFT may not capture correctly the detailed behavior in the brittle case just before localization when the dislocation density is very high in the localization region. Clarifying these details is subject of future numerical work.) After the system spanning fracture avalanche took place, continuous slip can be maintained at stresses that are $O(\varepsilon)$ less than the yield stress $F_c(\varepsilon)$. The corresponding stress-strain curve is shown in Fig. 2(a).

Results for slip hardening (*with* $\varepsilon < 0$, $\tau_{s,\ell} > \tau_{d,\ell}$).—Hardening can be introduced in this model in the following way: if a site slips the failure threshold of all other sites is either increased by an amount proportional to $|\varepsilon|/N$, or equivalently, the stresses at all cells are reduced by an amount $O(\varepsilon/N)$ [9]. In crystals, this global stress reduction or threshold strengthening may be due to the creation of dislocation pairs in the bulk that reduce the overall stress. This can lead to dislocation entanglement, so that higher stress than in nonhardening systems is needed to trigger further events [12]. From the general discussion of hardening in [1] we conclude that $|\varepsilon|/N$ is proportional to the hardening coefficient θ of the material. Starting from a relaxed state, for slowly increasing shear stress F, the system first responds with small avalanches, like in the $\varepsilon =$

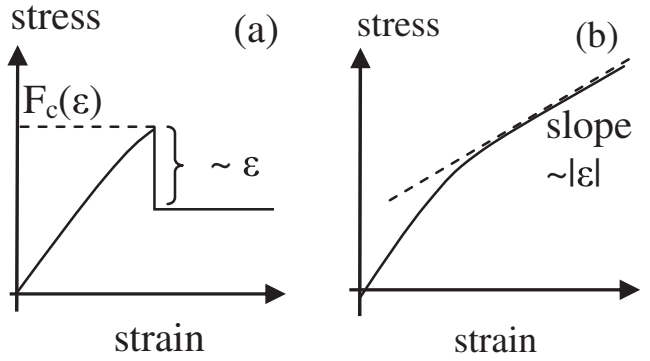

FIG. 2. Stress-strain curves for $\varepsilon > 0$ [(a) brittle] and $\varepsilon < 0$ [(b) hardening] as obtained from MFT.

0 case. During a transient regime, their size distribution $D(s, F, \varepsilon)$ follows the power law $1/s^{\tau}$ (with $\tau = 1.5$) up to a cutoff size that increases with F. For larger stresses, hardening effects come into play and the system crosses over into a ''steady state'' regime with a power law distribution of avalanche sizes that is cut off at maximum size $s_{\max} \sim 1/\varepsilon^2$, i.e. $D(s, F, \varepsilon) \sim 1/s^{\tau} D_h(s \cdot \varepsilon^2)$ with universal exponent $\tau = 1.5$ as before. As illustrated in Fig. 2(b), the slope of the stress-strain curve scales [1] as $G \sim 1/\langle s \rangle \sim |\varepsilon|$. In this regime the strain-rate power spectrum $P(\omega, F, \varepsilon)$ scales as $P(\omega, F, \varepsilon) \sim 1/\omega^2$ for high frequencies, with a low frequency cutoff $\omega_{\min} \sim \varepsilon$, i.e., the scaling form is given by $P(\omega, F, \varepsilon) \sim \omega^{-2} \mathsf{P}_h(\omega/\varepsilon)$. P_h is a universal scaling function. In the hardening regime, just as in the case for $\varepsilon = 0$, there is no slip localization, and the cumulative effect of all randomly nucleated avalanches is a distributed deformation of the solid.

Results for a small tangential velocity applied to the boundaries.—For this case, the mean field theory of the model becomes exactly as found for the BZR single fault earthquake model. It shows Gutenberg Richter (GR) power law statistics for $\varepsilon = 0$, characteristic earthquake distribution (with runaway events) for $\varepsilon > 0$, GR statistics with aftershocks for $\varepsilon < 0$, and mode switching between GR and characteristic earthquake distribution in a certain parameter regime for $\varepsilon < 0$ and in the absence of stress conservation [4,7–9].

Conclusions.—We have introduced a basic discrete model for solid deformation under two boundary conditions. For the case with applied shear stress, it is possible to tune the system by changing only one parameter (the weakening ε) from brittle ($\varepsilon > 0$), to ductile ($\varepsilon = 0$), and hardening ($\varepsilon < 0$) behavior. A continuous phase transition at $\varepsilon = 0$ separates brittle from hardening behavior. In the hardening phase the slip is on average uniformly distributed throughout the sample. In the brittle phase this holds only in the early deformation phase, before the slip localizes in a macroscopic failure event leading to breaking of the sample into two pieces. Our exact results for the universal scaling exponents characterizing this transition agree with recent experiments that found, for example, $\tau = 1.5$ [1,2]. Many of the predicted universal exponents and scaling functions computed in this Letter are yet to be measured in experiments. We find that the transition belongs to the same universality class as recently simulated models for dislocation dynamics, material damage, and earthquake statistics [1,4,5,7]. For slowly moving boundaries, the model displays the same behavior as the BZR earthquake model for a single heterogeneous fault that produces a variety of realistic results compatible with observations [4,7,8].

We thank N. Goldenfeld and J. Dantzig for useful discussions. K. D. thanks the Dept. of Earth Sciences at USC for kind hospitality and support. Y. B. Z. acknowledges support from the Southern California Earthquake Center, and K. D. from the Materials Computation Center [NSF DMR 03-25939 (MCC)].

[1] M. Zaiser, Adv. Phys. **55**, 185 (2006); F. Csikor *et al.*, Science **318**, 251 (2007); M. J. Alava *et al.*, Adv. Phys. **55**, 349 (2006); Y. Ben-Zion, Rev. Geophys. **46**, RG4006 (2008).

[2] T. Richeton *et al.*, Nature Mater. **4**, 465 (2005); D. M. Dimiduk *et al.*, Science **312**, 1188 (2006).

[3] M. C. Miguel and S. Zapperi, Science **312**, 1151 (2006), and references therein.

[4] D. S. Fisher, K. Dahmen, S. Ramanathan, and Y. Ben-Zion, Phys. Rev. Lett. **78**, 4885 (1997); Y. Ben-Zion and J. R. Rice, J. Geophys. Res. **98**, 14109 (1993); Y. Ben-Zion, M. Eneva, and Y. Liu, J. Geophys. Res. **108**, 2307 (2003).

[5] K. Chen *et al.*, Phys. Rev. A **43**, 625 (1991).

[6] Y. Ben-Zion, in *International Handbook of Earthquake and Engineering Seismology* (Academic Press, Boston, MA, 2003), Part B, Appendix 2, pp. 1857–1875.

[7] K. Dahmen and Y. Ben-Zion, *Encyclopedia of Complexity and System Science*, edited by C. Marchetti and R. Meyers (Springer, New York, 2009).

[8] K. Dahmen, D. Ertas, and Y. Ben-Zion, Phys. Rev. E **58**, 1494 (1998).

[9] A. P. Mehta, K. A. Dahmen, and Y. Ben-Zion, Phys. Rev. E **73**, 056104 (2006).

[10] J. P. Sethna, K. A. Dahmen, and C. R. Myers, Nature (London) **410**, 242 (2001); A. Travesset, R. A. White, and K. A. Dahmen, Phys. Rev. B **66**, 024430 (2002), and references therein.

[11] O. Narayan and D. S. Fisher, Phys. Rev. B **48**, 7030 (1993); G. Durin and S. Zapperi, *The Science of Hysteresis*, edited by G. Bertotti and I. Mayergoyz (Academic Press, Amsterdam, 2006), Vol. II, pp. 181–267, and references therein.

[12] L. Laurson and M. J. Alava, Phys. Rev. E **74**, 066106 (2006).